The Journal of Experimental Biology 210, 2352-2360
Published by The Company of Biologists 2007
doi:10.1242/jeb.004952

The effect of insect surface features on the adhesion of viscous capture threads spun by orb-weaving spiders

Brent D. Opell[1,*] and Harold S. Schwend[2]

[1]*Department of Biological Sciences and* [2]*College of Veterinary Medicine, Virginia Polytechnic Institute and State University, Blacksburg, VA 24061, USA*

*Author for correspondence (e-mail: bopell@vt.edu)

Accepted 24 April 2007

Summary

Spider orb-webs intercept a broad range of insects and their capture threads must adhere to a range of surface textures. In species of the Araneoidea clade, these capture threads are composed of viscid droplets whose size and spacing differ among species. To determine how droplet profile and insect surface texture interact, we measured the stickiness of viscous threads produced by four species using four insect surfaces that ranged from a smooth beetle elytra to the dorsal surface of a fly abdomen that was covered by large, widely spaced setae. The adhesion of threads to these surfaces differed by as much as 3.5-fold within a spider species and 2.1-fold for the same insect surface between spider species. However, 96% of these differences in stickiness was explained by four variables: the ratio of natural log of droplet volume to setal length, the natural log of droplet volume per mm of thread length, setal surface area, and the area of cuticle not excluded from thread contact by setae. Compared with previous measurements of primitive cribellar capture threads produced by orb weavers of the Deinopoidea clade, viscous threads performed more uniformly over the range of insect surfaces. They also held bug hemelytra, which were densely covered with fine setae, more securely, but held beetle elytra, fly wings and fly abdomens less securely than did viscous threads. Hemelytra may be held more securely because their setae more easily penetrate the viscous boundary layer to establish a greater area of interaction and, after having done so, offer more resistance as they are pulled through this layer. Finely textured surfaces may also have higher effective surface energies and therefore may interact more completely with viscous material.

Key words: cribellar thread, spider thread adhesion, prey capture, orb-web.

Introduction

Many factors affect the broad range of prey that spider orb-webs intercept, including insect availability (Reichert and Cady, 1983; Wise and Barata, 1983; Craig, 2003), web area (Eberhard, 1986), web orientation (Eberhard, 1989; Eberhard, 1990), web invisibility or attractiveness to insects (Blackledge, 1998a; Blackledge, 1998b; Blackledge and Wenzel, 1999; Craig and Bernard, 1990; Craig et al., 1994), the presence of a stabilimentum at the center of the web (Herberstein et al., 2000), and the visibility of a spider positioned at the web's hub (Blackledge, 1998a; Blackledge, 1998b; Blackledge and Wenzel, 1999; Craig and Ebert, 1994; Zschokke, 2002). However, unless insects remain in the web long enough for a spider to locate, run to and subdue them, their interception is of no benefit to a spider. When a spider is removed from its orb-web, only very small insects remain in the web for more than a few hours (Opell et al., 2006). By retaining insects, an orb-web's spirally arrayed, sticky capture threads play a crucial role in this latter phase of prey capture (Chacón and Eberhard, 1980; Eberhard, 1990; Wise, 1993).

The most commonly encountered orb-weaving spiders belong to the large Araneoidea clade, whose members spin viscous capture threads. These composite threads are spun from the spigots of two adjacent silk glands (Foelix, 1996). The flagelliform glands produce a pair of supporting axial fibers and the aggregate glands coat these fibers with a viscous, aqueous solution that quickly forms into droplets (Gosline et al., 1984; Peters, 1986; Peters, 1995; Vollrath et al., 1990). The glycoprotein granules that coalesce inside each droplet contribute to thread adhesion (Vollrath and Tillinghast, 1991; Tillinghast et al., 1993) and the hydrophilic compounds in the surrounding fluid attract atmospheric moisture to prevent droplets from drying (Vollrath et al., 1990; Townley et al., 1991). The elasticity of the thread's axial fibers and the plasticity of its droplets comprise an effective mechanism for summing the adhesion generated by multiple droplets (Opell and Hendricks, 2007).

Previous studies of viscous threads have used either smooth acetate (Opell and Hendricks, 2007) or fine sandpaper (Opell, 1997; Opell, 1998; Opell, 1999a; Opell, 2002) surfaces to

measure the stickiness of viscous capture threads. In this study we used four insect surfaces whose setae differ greatly in size and density to measure the stickiness of four species' viscous threads whose droplet size and spacing differ markedly. This comparison offers a perspective on how viscous threads perform across a range of insect surfaces and provides data for modeling this interaction. Moreover, as we used insect surfaces of the same texture that were used previously to measure the stickiness of primitive cribellar capture threads (Opell, 1994a) constructed by orb-weavers of the Deinopoidea clade, the sister clade of the Araneoidea (Coddington, 1986; Coddington, 1989; Griswold et al., 1998; Garb et al., 2006), we are able to compare the performance of these two types of capture thread.

We hypothesize that three factors determine the stickiness of a viscous thread: the amount of viscous material it presents to a surface, the total area of an insect's surface with which viscous threads interact, and the nature of this interaction. Contact area differs greatly among insect surfaces, as it comprises both cuticular area and the surface areas of setae extending from the cuticle. Moreover, large setae can prevent viscous material from contacting an insect's cuticle and provide the only surfaces of contact. Even the bases and shafts of minute setae can exclude small amounts of viscous material from contacting an insect's cuticle.

Cribellar and viscous capture threads interact differently with surfaces and generate their adhesion by different mechanisms (Opell and Hendricks, 2007). The outer surfaces of cribellar threads are formed of thousands of fibrils, each with a diameter of around 20 nm (Peters, 1984; Eberhard and Pereira, 1993; Opell, 1994b; Hawthorn and Opell, 2002; Hawthorn and Opell, 2003). These fibrils implement mechanical interlock to snag on insect setae and irregular surfaces (Opell, 1994a) and additional mechanisms to adhere to smooth surfaces. Fibrils of all but the most primitive cribellar threads feature regularly spaced, 35 nm diameter nodes that establish as many as 170 points of interaction with each μm^2 of surface they contact (Hawthorn and Opell, 2003). At low relative humidity (RH) each of these nodes generates van der Waals forces, but at a RH of 45% or greater they generate stronger capillary forces (Hawthorn and Opell, 2003). By contrast, the droplets of viscous threads spread over surfaces they contact and adhesion is generated over a greater, more continuous surface area. Whereas cribellar threads generate useful adhesion principally at edges of contact with a surface, viscous threads recruit the adhesion generated by multiple contacting droplets (Opell and Hendricks, 2007).

These differences in adhesive mechanisms and delivery systems contribute to differences in the efficiencies of cribellar and viscous threads. Relative to their material volumes, viscous threads generated greater adhesion than cribellar threads when their stickiness was measured with fine sandpaper (Opell, 1998), a surface that registered stickiness values similar to that of fly wings (Opell, 1994c; Opell, 1997). However, of four insect surfaces with well-attached setae, cribellar thread registered the lowest value when measured with fly wings (Opell, 1994a) and the greatest values when measured with two extremely different surfaces: beetle elytra with the largest proportion of exposed waxy cuticle and fly nota with large, widely spaced setae. Beetle elytra appear to offer maximal opportunity for cribellar threads to adhere by capillary action, whereas fly nota offer maximal opportunity for cribellar fibrils to interlock with setae. A bug hemelytra, which was covered with very small, densely packed setae, and fly wing, which was covered by somewhat larger, more widely spaced setae, registered intermediate stickiness values.

We hypothesize that viscous threads will perform differently on these surfaces. For example, a hemelytra's small, dense setae should optimize interactions with viscous droplets by penetrating the surface of droplets and, thereby, increasing the area of contact or by conferring higher surface energy that increases the interaction with viscous material. By contrast, the large setae on fly nota and abdomens probably prevent viscous droplets from contacting underlying cuticle, and limit the surface area that contacts viscous material. An understanding of how viscous threads interact with a range of insect surface textures will provide a more complete picture of the performance of these threads and the prey-capture webs that they form.

The four araneoid species that we studied belong to the family Araneidae and can be found near one another. However, they have different microhabitats, body sizes, web sizes and web features (Table 1). *Araneus marmoreus* Clerck and *Argiope tirfasciata* (Forskål) are large spiders that build large webs with widely spaced spirals. *A. marmoreus* places its web 1.5–2.0 m above the ground on trees and shrubs at the forest edge. Unlike the other three species that rest at the center of

Table 1. *Adult female size and web characteristics of the four araneoid species studied*

	Cyclosa turbinata (*N*=23)	*Micrathena gracilis* (*N*=21)	*Argiope trifasciata* (*N*=25)	*Araneus marmoreus* (*N*=15)
Spider mass (mg)	8.9±0.8	84.3±5	474.0±51.6	677.1±75
Web capture area (cm^2)	92±7	201±12	848±74	600±42
Spiral spacing (mm)	1.6±0.1	1.3±0	3.9±0.2	3.1±0.2
Stickiness per capture area ($\mu N/cm^2$)	855±37	2333±75	778±39	1307±76

Values are means ± 1 s.e.m. (from Opell, 1999b).

Capture area is the area of the web bounded by the innermost and outermost capture spiral turn. Thread stickiness was measured with fine sandpaper, which registers stickiness that is very similar to that of a fleshfly wing (Opell, 1997).

their webs, *A. marmoreus* monitors its web from adjacent vegetation where it constructs a retreat from a curled leaf. *A. tirfasciata* is found in weedy patches and along fence rows where it builds webs at heights of 0.5–1.5 m. *Cyclosa turbinata* (Walckenaer) is a small spider that builds small webs with closely spaced spirals. It is found in many exposed sites and builds webs 0.5–1.5 m above the ground. *Micrathena gracilis* (Walckenaer) is of intermediate size and constructs webs of intermediate diameter that have very closely spaced spirals. It is found in forests, where its webs are usually suspended 1.0–1.5 m above the ground by long framework lines. Unlike the other three species, whose webs are vertically oriented, those of *M. gracilis* can have a vertical to nearly horizontal orientation. These differences in microhabitat, capture spiral spacing and web placement probably result in the four species capturing different subsets of the insects. However, as most orb-weaving spiders are generalist predators that capture a range of insects (Eberhard, 1990; Wise, 1993), the webs of each of these four species encounter insects with a range of surface textures. The insect surfaces that we used were selected to reflect this range of textures. Although orb-webs of the four species that we studied intercept dipterans, hemipterans and coleopterans, we have no information about the relative contribution of these taxa to their diets.

Materials and methods

Species studied and thread collection

We collected viscous capture threads from newly spun orb-webs constructed by adult females found in Montgomery Co., VA, USA. We collected threads on samplers made by gluing 4.8 mm square brass supports at 4.8 mm intervals to microscope slides. Double-sided tape on the supports held thread strands securely at their native tension. The photographs of each individual's threads were taken and all stickiness measurements were made under the same RH and temperature within 6.5 h after threads were collected. Sample size denotes the number of spiders from whose webs threads were taken.

Droplet measurements

Using techniques described more fully elsewhere (Opell and Hendricks, 2007) we photographed the threads of each species and measured these digital images with ImageJ (ImageJ, 2006) to characterize the size and spacing of their primary droplets (Table 2). Threads spun by some individuals also had smaller secondary droplets between some of their primary droplets. As the total volume of these secondary droplets was small (Table 2) and their presence and size was variable, we included only the primary droplets in this study. As droplet profile best matched that of a parabola, we determined droplet volume (DV) using the following formula generated from the formula of a parabola rotated around its *x*-axis (Opell and Hendricks, 2007):

$$DV = (2\pi \text{ droplet width}^2 \times \text{droplet length}) / 15 .$$

Insect surface features

Each species' threads were measured with four insect surfaces (Figs 1–4): (1) the dorsal surface of a fleshfly (*Sarcophage bullata* Parker) abdomen, (2) the upper surface of a fleshfly wing, (3) the distal portion of the hemelytra of a milkweed bug [*Oncopeltus fasciatus* (Dallas)], and (4) the elytra of a convergent lady beetle (*Hippodamia convergens* Gurin-Meneville). These surfaces were chosen to provide a broad range of textures and to match the surfaces used previously to compare the stickiness of the cribellar capture threads (Opell, 1994a). We chose a fleshfly abdomen rather than a notum, as used to measure cribellar threads (Opell, 1994a), because the abdomen provided a larger, flatter piece of cuticle. However, these two surfaces have very similar setal characteristics [Fig. 1; fig. 1f in Opell (Opell, 1994a)].

We killed insects by freezing at –80°C for 5–10 min, immediately removed the surfaces to be used for measuring stickiness, placed them in covered Petri dishes, and kept them

Table 2. *Thread features of the four species studied*

	Cyclosa turbinata	*Micrathena gracilis*	*Argiope trifasciata*	*Araneus marmoreus*
Droplet length (μm)	12.42±0.69	28.83±2.59	44.20±1.87	62.92±4.89
Droplet width (μm)	9.42±0.45	21.11±2.19	27.37±1.80	47.22±3.66
Volume ($\mu m^3 \times 10^2$)	7.28±0.92	82.02±25.38	250.78±30.08	1012.18±195.15
Droplets mm^{-1}	26.24±2.47	12.87±2.99	5.85±0.65	4.39±0.38
$\log_N$ primary droplet volume ($mm^2\ mm^{-1}$)	9.7133	11.4781	11.7794	12.7255
Percent secondary droplet volume	10.8	8.18	8.9	5.4
Proportional droplet spacing	2.40	0.52	0.16	0.08
Volume ($mm^3\ mm^{-1}$)	0.018±0.002	0.110±0.036	0.140±0.019	0.387±0.061
Relative droplet size:				
abdomen	0.0074	0.0165	0.0207	0.0259
wing	0.0794	0.1763	0.2210	0.2768
hemelytra	1.7113	3.7991	4.7626	5.9654
elytra	0.3059	0.6790	0.8512	1.0662

Values are means ± 1 s.e.m.; *N*=10 except for *M. gracilis* (*N*=3).
Sample size (*N*) denotes the number of spiders from whose webs threads were taken.

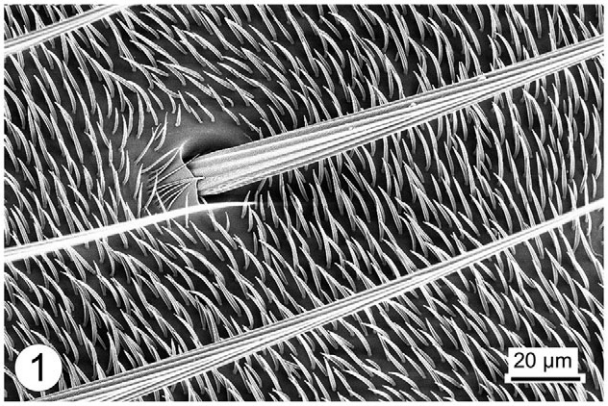

Fig. 1. The dorsal surface of a fleshfly (*Sarcophage bullata*) abdomen.

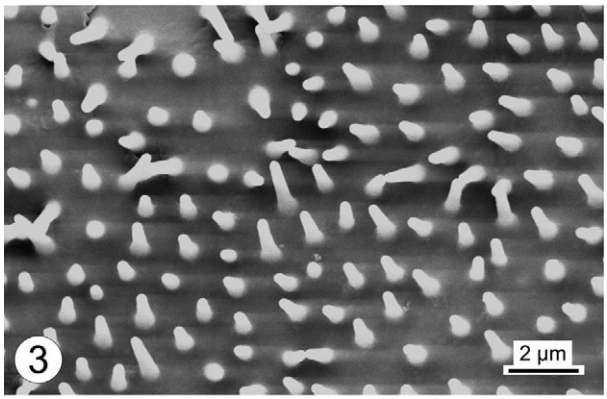

Fig. 3. The distal portion of the hemelytra of a milkweed bug (*Oncopeltus fasciatus*).

in a desiccator until used. Each surface was affixed to a 1891 μm-wide (N=16, s.d.=22 μm) brass plate with water-based latex adhesive (Polymark™ fabric and craft paint) and trimmed to the plate width with a razor blade before use. Beetle elytra could not be trimmed to create a clean edge and, therefore, were used as removed. The mean width of the elytra mid-region that was used to measure stickiness was 2058 μm (N=10, s.d.=2 μm). To account for this slightly greater width, we multiplied the stickiness measured with elytra by 0.91885.

We measured setal characteristics of nine specimens per insect species. These surfaces were sputter-coated with gold palladium and photographed under a Leo scanning electron microscope (SEM) (Figs 1–4). We used ImageJ to determine the size and distribution of the setae on these surfaces. Setal size was based on the lengths and widths of three setae from each sample and setal density on the number of setae in three regions of each sample.

Stickiness measurements

We covered contact plates with the four insect surfaces and measured three thread strands from each spider web with each surface. An insect surface was replaced after three strands were measured, ensuring that a thread always contacted an unused sector of the insect surface. The mean value registered by these three strands was used as a spider's value for that insect surface. Immediately before measuring the stickiness of individual thread strands, we measured ambient temperature, humidity and barometric pressure.

Stickiness was measured with an instrument [illustrated and described in detail by Opell and Hendricks (Opell and Hendricks, 2007)] that incorporated interchangeable contact plates attached to the lever arm of a jeweled escapement, which transferred force to a load cell that was machined to increase its sensitivity. A linear actuator pressed the thread against a contact plate at a speed of 0.06 mm s^{-1} until a force of 25 μN was generated, at which time the direction of travel was immediately reversed. As the strand was withdrawn, its adherence to the plate exerted force on the plate and the maximum force achieved before the strand pulled free of the plate was recorded as the strand's stickiness.

Comparison of viscous and cribellar thread adhesion

It has been established that, relative to its material volume, viscous thread is stickier than cribellar thread (Opell, 1998). Therefore, we based our comparisons of the performance of the two types of threads on the relative stickiness that each type

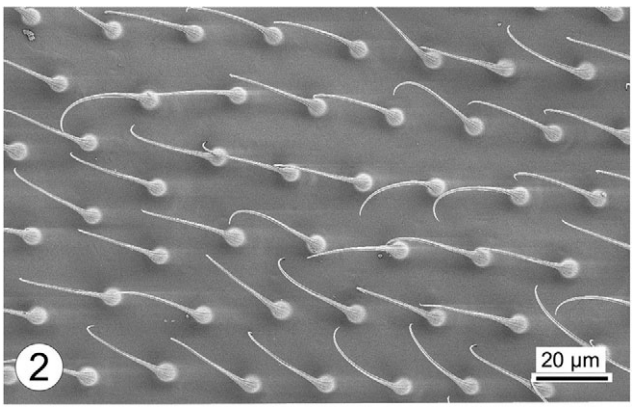

Fig. 2. The upper surface of a fleshfly wing.

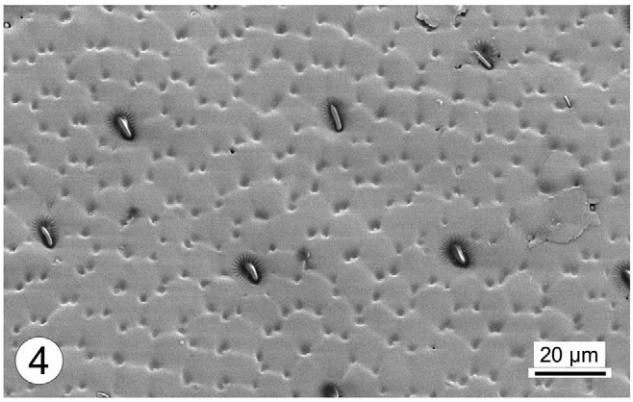

Fig. 4. Elytra of a convergent lady beetle (*Hippodamia convergens*).

registered on the four insect surfaces. For each thread type, we divided the mean stickiness that each species' thread registered on a particular surface by the mean stickiness expressed on the surface that generated the greatest adhesion. Then we determined the mean relative stickiness registered on each surface by threads of the four species included in this study and by the two cribellate species from the earlier study (Opell, 1994a). In this latter study, only one species' threads were measured using the hemelytra.

Statistical analysis and modeling

We used the S.A.S. statistical package (S.A.S. Institute Inc., Cary, NC, USA) to test the normality of data, compare stickiness values and develop regression models that used thread and insect surface features to explain stickiness. We identified five indices that promised to be related to thread stickiness: two indices that described the features of capture thread, two that described the features of insect surfaces, and one that described the interaction of thread and insect surfaces.

Natural log of the volume of viscous material per mm length of capture thread (LVPMM)

A positive relationship was previously identified between thread stickiness, as measured with contact plates covered with fine sandpaper, and LVPM (Opell, 2002).

Proportional droplet spacing (PDS)

The mean spacing between droplets divided by mean droplet dimensions, the average of droplet length and droplet width.

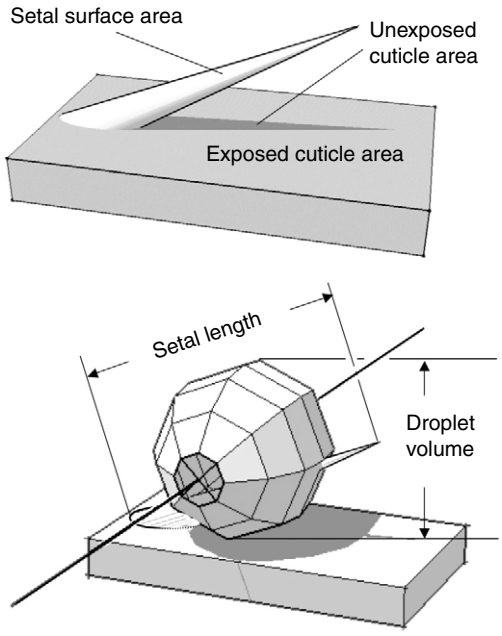

Fig. 5. Values used in modeling the interaction between viscous threads and insect surfaces.

Setal surface area (SSA)

The setal area in each mm^2 of insect surface available to interact with viscous thread. For the tapered setae of fly abdomens, fly wings and beetle elytra we computed setal area as the area of a cone, as described by the formula:

$$\text{SSA} = (\pi \text{ setal radius} \sqrt{\text{setal radius}^2 + \text{setal length}^2}) - \pi \text{ setal radius}^2 .$$

We computed the surface area of the more cylindrical setae of hemelytra as the area of a cylinder capped by a circle using the formula:

$$\text{SSA} = (\pi \text{ setal diameter} \times \text{setal height}) + (\pi \text{ setal radius}^2) .$$

Exposed cuticle area (ECA)

The area in each mm^2 of insect surface that is not blocked from thread contact by setae. For the angled, conical setae of fly wings and beetle elytra, we compute ECA by subtracting from 1 mm^2 the total area of the triangular 'shadows' of setae (Fig. 5) found in each mm^2 of insect surface using the formula:

$$\text{ECA} = 1 \text{ mm}^2 - [(\text{setae mm}^2)^{-1} \times (\text{setal width} \times \text{setal length}/2)] .$$

For the perpendicular, cylindrical setae of hemelytra, we computed ECA by subtracting the circular shadows (=setal cross-sectional areas) of the seate in each mm^2 of insect surface using the following formula:

$$\text{ECA} = 1 \text{ mm}^2 - [(\text{setae mm}^2)^{-1} \times (\pi \text{ setal radius}^2)] .$$

For the fly abdomen we used an ECA value of zero. Unlike the other insect surfaces, the very large setae on the fly's abdomen are underlain by small, closely spaced setae (Fig. 1). We believe that when viscous threads contact these large setae they are suspended above these smaller setae and, therefore, do not contact either these setae or the underlying cuticle.

Total contact area (TCA)

The sum of SSA and ECA.

Relative droplet size (RDS)

The natural log of DV divided by setal length (Fig. 5).

Results

Viscous thread stickiness

Mean stickiness ranged from 30–105 μN, a 3.6-fold difference (Table 3, Fig. 6). The grand mean stickiness values registered by the four species' threads on the four insect surfaces were: hemelytra 87.0 μN, elytra 44.3 μN, wing 39.5 μN, and abdomen 33.2 μN. Of the 16 stickiness values registered by the four species' threads on the four insect surfaces, only 11 were normally distributed (Shapiro–Wilk *W*-statistic test, $P>0.05$). However, the natural log of the stickiness was normally distributed for all values except the stickiness registered by *M. gracilis* threads on beetle elytra. A

Table 3. *Stickiness values, and the temperature, barometric pressure and relative humidity under which they were measured*

	Stickiness (μN)				Temperature	BP	
	Fly abdomen	Fly wing	Bug hemelytra	Beetle elytra	(°C)	(mmHg)	%RH
Cyclosa turbinata	28.21±1.79	33.04±3.14	51.71±7.16	30.06±1.29	22.8±0.2	1017±1	$36.5±3.8^{B}$
Micrathena gracilis	43.93±8.08	39.26±3.59	82.83±7.67	47.98±9.53	23.7±0.3	1018±2	$52.8±1.3^{A}$
Argiope trifasciata	30.55±2.39	40.51±4.19	107.88±16.26	46.50±2.40	22.4±0.3	1015±1	$43.2±3.6^{A,B}$
Araneus marmoreus	30.24±3.67	45.18±5.33	105.54±23.48	52.64±5.04	23.5±0.4	1016±1	$53.4±1.6^{A}$

Values are means ± 1 s.e.m.; *N*=10 except for *M. gracilis* (*N*=3).
BP, barometric pressure (1 mmHg=133.32 Pa); RH, relative humidity.
Superscripts beside mean RH denote the ranking assigned by a Ryan–Einot–Gabriel–Welsch Multiple Range Test.

two-factor analysis of variance (ANOVA) (F=23.11, P=0.0001) showed that $\log_N$ thread stickiness was affected by both species and insect surface type (P=0.0001 for each factor). Insect surface affected the $\log_N$ stickiness of each species' thread (ANOVA P for *A. marmoreus*, *A. trifasciata*, *M. gracilis* and *C. turbinate*: 0.0001, 0.0001, 0.0470 and 0.0003, respectively). The rank of each species' values, as assigned by a Ryan–Einot–Gabriel–Welsch Multiple Range Test (α=0.05), is presented in Fig. 6.

Model of thread stickiness

The droplet features and insect surface features used to compute the four contributing indices (LVPMM, SSA, ECA and RDS) are given in Table 2 and Table 4. These indices were each directly related to stickiness (P=0.0001) but PDS was not (P=0.13). In a composite model that excluded PDS, the four remaining variables were directly related to stickiness ($P \leqslant 0.0002$) and produced the following model (P=0.0001, R^2=0.96):

$$\text{Stickiness} = 2.8158\ \text{LDVPMM} + 2.7620\ \text{SSA} + 4.8815\ \text{ECA} + 11.7764\ \text{RDS} - 0.696\ .$$

A model that replaced SSA and ECA with TCA performed equally well (P=0.0001, R^2=0.96):

$$\text{Stickiness} = 2.9883\ \text{LDVPMM} + 4.7118\ \text{TCA} + 11.3805\ \text{RDS} - 3.0279\ .$$

A maximum R^2 improvement analysis (P for entry=0.01) added variables to the model in the following sequence: RDS (R^2=0.9437), LDVPMM (R^2=0.9542), ECA (R^2=0.9568), SSA (R^2=0.9573). When RDS was removed, the fitnesses of the resulting three- and two-variable models decreased but were still robust (P=0.0001, R^2=0.84 and P=0.0001, R^2=0.82, respectively). In the three-variable model, the contribution of SSA was greater than that of ECA, and produced the following formula:

$$\text{Stickiness} = 7.9473\ \text{LDVPMM} + 40.0927\ \text{SSA} + 29.649815\ \text{ECA} - 80.8322\ .$$

The temperature and barometric pressure under which the four species' stickiness measurements were made (Table 3) did not differ (ANOVA P=0.07 and 0.39, respectively), although RH did (P=0.003), principally because threads of *C. turbinata* were measured at lower RH. However, RH was not related to thread stickiness, either alone (P=0.28) or when added to the four-variable model of stickiness (P=0.64).

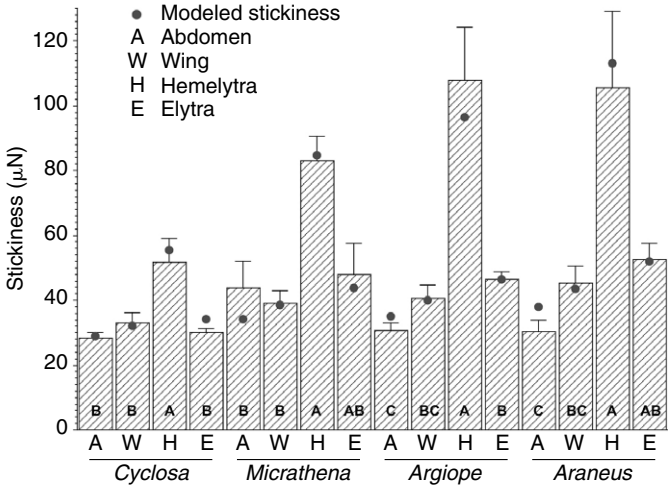

Fig. 6. Comparison of the measured and modeled stickiness that four species' viscous threads registered on contact plates covered with four insect surfaces. Histogram bars denote measured stickiness with error bars of ±1 s.e.m. Letters denote the ranking (high to low) of each species' measured values as determined by Ryan–Einot–Gabriel–Welsch Multiple Range Tests. Dots represent stickiness values determined by the four-variable model.

The effect of setal angle

Our computation of ECA accounted for setal angle by computing the setal 'shadow' of the angled setae on fly wings and beetle elytra as triangles and of the nearly perpendicular setae of hemelytra as circles. However, further attempts to analyze the effect of setal angle were inconclusive. As the setae on fly abdomens and wings were curved, their angle with the cuticle changed over their lengths, becoming less acute towards the tip. The angles of setae on the third abdominal segment of the fly abdomen were more acute than those on the second sclerite. The abdomen is unique in having very large setae that prevent threads from contacting the underlying cuticle.

Table 4. *Insect surface features (mean ± 1 s.e.m.)*

	Fly abdomen	Fly wing	Bug hemelytra	Beetle elytra
Setal width (mm) (*N*=9)	8.54±0.60	1.21±0.05	0.44±0.02	1.21±0.06
Setal length (mm) (*N*=9)	267.23±17.09	25.00±1.40	1.16±0.15	6.49±0.37
Setae per mm^2 (*N*=9)	99.4±5.4	2716.1±206.6	709876.5±42138.4	432.1±113.8
Setal surface area (mm^2/mm^2)	0.5747	0.1748	1.2458	0.0049
Exposed cuticle area (mm^2/mm^2)	0	0.9424	0.8921	0.9983
Total contact area (mm^2/mm^2)	0.5747	1.1172	2.1379	1.0032

Moreover, estimates of setal angles made from SEM images and dissecting microscope examination (abdomen 40°, wing 40°, hemelytra 90° and elytra 5°) were highly correlated with SSA (R=0.94, P=0.0001). By contrast, the only other correlated indices, SSA and RDS, had a lower value (R=0.75, P=0.0009), with all other indices being uncorrelated (P>0.21). Therefore, we do not believe that our data permit us to make useful conclusions about the effect of setal angle on viscous thread adhesion.

Comparison of viscous and cribellar thread stickiness

For each of the four insect surfaces, the relative stickiness of both viscous and cribellar threads was normally distributed (Shapiro–Wilk W-Statistic $P \geqslant 0.05$). Relative stickiness differed among both viscous and cribellar threads (P<0.0011) and Ryan–Einot–Gabriel–Welsch Multiple Range Tests ranked these values as shown in Fig. 7. Viscous threads registered the greatest values on hemelytra, but the values obtained with the other three surfaces were similar. By contrast, cribellar threads registered the greatest value on the elytra, followed by the notum (abdomen), hemelytra and wing.

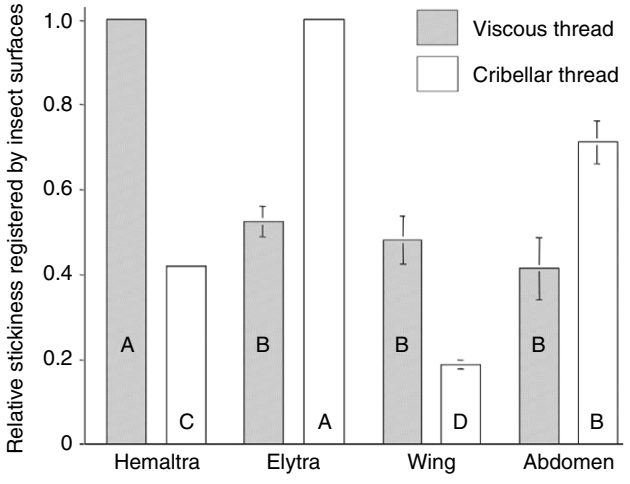

Fig. 7. Comparison of the relative stickiness values of viscous and cribellar threads. Error bars represent ± 1 s.e.m. Letters denote the separate rankings (high to low) of mean values of viscous and cribellar threads on each of the four insect surfaces as determined by Ryan–Einot–Gabriel–Welsch Multiple Range Tests.

Discussion

The volume of viscous material per mm thread length differed by as much as 22-fold among the four species' threads. The length of setae on the four insect surfaces differed by as much as 230-fold and their densities by as much as 7170-fold. Measured stickiness differed by as much as 3.5-fold within a species and 2.1-fold between species for the same insect surface. However, a model based on four variables, LDVPMM, SSA, ECA and RDS, explained 96% of the difference in stickiness among the 16 combinations of threads and insect surfaces. Combining the two surface area measurements, SSA and ECA, produced a three-variable model of equal fitness. This high fitness indicates that the composition of the four species' viscous droplets and the surface energies of the four insect surfaces are either more similar than might be expected or that these characteristics have less effect on adhesion than do the dynamics of interactions between setae and viscous droplets.

Setae play a crucial role by increasing the surface area that interacts with viscous material, as is evident from the actual surface area per mm^2 of insect cuticle (Table 4). Smooth beetle elytra have an effective area of 1.003 mm^2 per mm^2, whereas the fly wing and hemelytra had effective areas of 1.117 and 2.138 mm^2 per mm^2, respectively. However, setae also appear to have a qualitative effect upon adhesion, as shown in the model comprised of LDVPMM, SSA and ECA, in which the effect of SSA was 1.38 times that of ECA. Moreover, RDS alone was directly related to adhesion and explained 94% of the observed stickiness. This index, which increases as DV increases relative to setal length, appears to characterize the interaction between setae and viscous material. For all species RDS is greatest for hemelytra, where droplets engulf a large number of setae when they flatten. RDS is smallest for fly abdomens, where the mean length of even the largest viscous droplets (those of *A. marmoreus*) is only approximately 20% of the length of setae (Tables 2, 4). Compared with large setae, those that are small relative to viscous droplets may more easily penetrate the viscous boundary layer to establish a greater area of interaction and, after doing so, offer more resistance as they are pulled through viscous material. Finely textured surfaces may also have higher effective surface energies and thereby interact more completely with viscous material. If capillary force contributes to droplet adhesion, it would also be enhanced by this increased surface energy (Israelachvili, 1992).

As hypothesized, the relative stickiness values that viscous

and cribellar threads registered on insect surfaces differed (Fig. 7). These differences are explained by differences in the adhesive mechanisms of the two thread types and by the interaction of these threads with insect setae and are profiled by three contrasts. The first is the performance of fly abdomens or nota that registered one of the three lowest stickiness values for viscous threads and the greatest stickiness for cribellar threads. The long, widely spaced setae on these surfaces presented only a small surface area for viscous droplets to contact, and they prevented viscous threads from contacting the smaller, more closely spaced underlying setae (Fig. 1). Had droplets contacted these smaller setae, viscous threads would probably have registered stickiness values intermediate between those registered by fly wings and bug hemelytra. By contrast, cribellar fibrils snagged the large setae and perhaps also some of the small, underlying setae on fly nota, permitting cribellar threads to hold to this surface by mechanical interlock (Opell, 1994a; Hawthorn and Opell, 2002; Hawthorn and Opell, 2003).

The second contrast is seen in the performance of bug hemelytra, which registered the greatest absolute and relative stickiness when measured with viscous threads and next to the lowest stickiness when measured with cribellar threads. As noted above, the hemelytra's covering of minute setae optimize surface interactions with viscous droplets. By contrast, cribellar fibrils probably contact principally the tips of these setae where they generate capillary forces [the dominant adhesive force at the humidity under which these measurements were made (Hawthorn and Opell, 2002; Hawthorn and Opell, 2003)] and have little opportunity to contact the underlying cuticle or to implement mechanical interlock.

The third contrast is seen in the performance of beetle elytra, which registered approximately twice the relative stickiness for cribellar thread as it did for viscous thread. The elytra's small, sparse setae lie in cuticular grooves (Fig. 4) and present a flat surface to threads that should establish extensive cuticluar contact and minimize the opportunity for setal interactions. The presumably low surface energy of this waxy surface may account for the low adhesion of viscous thread, but it should also limit the ability of cribellar fibrils to generate capillary forces (Israelachvili, 1992; Hawthorn and Opell, 2003). Therefore, greater relative stickiness registered by cribellar threads is most easily explained by mechanical interlock of cribellar fibrils with elytral setae, which are more likely to snag cribellar fibrils, as they are 5.6 times the lengths of hemelytral setae and extend at more oblique angles from the cuticle.

Although important, surface-specific capture thread adhesion is only one factor that determines how long an orb-web retains insects. Other factors include how many capture threads a prey strikes, whether or not these threads break on initial impact or wrap around a struggling insect. Investigations of these factors remain to be performed. The wings and dorsal region of a struggling insect are not the only surfaces that contact the web's capture threads. However, these surfaces comprise a large portion of the insect's body surface and are clearly surfaces that must be pulled free of the capture spirals if the insect is to escape the web. This study shows that the surface features of an insect body determine how much of a capture thread's potential adhesion contributes to insect retention. This operational thread adhesion combines with features of web architecture, such as capture spiral spacing, and with a spider's running speed and mode of prey immobilization to determine how securely insects are held by a web and which are most likely to be captured by a spider.

Mary Hendricks, D. Michael Leonard and Lindsay Neist helped with field and laboratory work. Cara Cherry and Mary Hendricks provided helpful comments on the manuscript. National Science Foundation grant IOB-0445137 supported this research.

References

Blackledge, T. A. (1998a). Signal conflict in spider webs driven by predators and prey. *Proc. R. Soc. Lond. B Biol. Sci.* **265**, 1991-1996.

Blackledge, T. A. (1998b). Stabilimentum variation and foraging success in *Argiope aurantia* and *Argiope trifasciata* (Araneae, Araneidae). *J. Zool.* **246**, 21-27.

Blackledge, T. A. and Wenzel, J. W. (1999). Do stabilimenta in orb-webs attract prey or defend spiders. *Behav. Ecol.* **10**, 372-376.

Chacón, P. and Eberhard, W. G. (1980). Factors affecting numbers and kinds of prey caught in artificial spider webs with considerations of how orb-webs trap prey. *Bull. Br. Arachnol. Soc.* **5**, 29-38.

Coddington, J. A. (1986). The monophyletic origin of the orb-web. In *Spiders: Webs, Behavior and Evolution* (ed. W. A. Shear), pp. 319-363. Stanford: Stanford University Press.

Coddington, J. A. (1989). Spinneret silk spigot morphology: evidence for the monophyly of orb-weaving spiders, Cyrtophorinae (Araneidae), and the group Theridiidae plus Nesticidae. *J. Arachnol.* **17**, 71-96.

Craig, C. L. (2003). *Spider Webs and Silk: Tracing Evolution from Molecules to Genes to Phenotypes.* New York: Oxford University Press.

Craig, C. L. and Bernard, G. D. (1990). Insect attraction to ultraviolet-reflecting spider webs and web decorations. *Ecology* **71**, 616-624.

Craig, C. L. and Ebert, K. (1994). Color and pattern in predator-prey interactions: the bright body colors and patterns of tropical orb-weaving spiders attract flower-seeking prey. *Funct. Ecol.* **8**, 616-620.

Craig, C. L., Bernard, G. D. and Coddington, J. A. (1994). Evolutionary shifts in the spectra properties of spider silks. *Evolution* **48**, 287-296.

Eberhard, W. G. (1986). Effect of orb-web geometry on prey interception and retention. In *Spiders: Webs, Behavior, and Evolution* (ed. W. A. Shear), pp. 70-100. Stanford: Stanford University Press.

Eberhard, W. G. (1989). Effects of orb-web orientation and spider size on prey retention. *Bull. Br. Arachnol. Soc.* **8**, 45-48.

Eberhard, W. G. (1990). Function and phylogeny of spider webs. *Annu. Rev. Ecol. Syst.* **21**, 341-372.

Eberhard, W. G. and Pereira, F. (1993). Ultrastructure of cribellate silk of nine species in eight families and possible taxonomic implications (Araneae: Amaurobiidae, Deinopidae, Desidae, Dictynidae, Filistatidae, Hypochilidae, Stiphidiidae, Tengellidae). *J. Arachnol.* **21**, 161-174.

Foelix, R. F. (1996). *Biology of Spiders* (2nd edn). New York: Oxford University Press.

Garb, J. E., DiMauro, T., Vo, V. and Hayashi, C. Y. (2006). Silk genes support the single origin of orb-webs. *Science* **312**, 1762.

Gosline, J. M., Denny, M. W. and Demont, M. E. (1984). Spider silk as rubber. *Nature* **309**, 551-552.

Griswold, C. E., Coddington, J. A., Hormiga, G. and Scharff, N. (1998). Phylogeny of the orb-web building spiders (Araneae, Orbiculariae: Deinopoidea, Araneoidea). *Zool. J. Linn. Soc.* **123**, 1-99.

Hawthorn, A. C. and Opell, B. D. (2002). Evolution of adhesive mechanisms in cribellar spider capture thread: evidence for van der Waals and hygroscopic forces. *Biol. J. Linn. Soc. Lond.* **77**, 1-8.

Hawthorn, A. C. and Opell, B. D. (2003). van der Waals and hygroscopic forces of adhesion generated by spider capture threads. *J. Exp. Biol.* **206**, 3905-3911.

Herberstein, M. E., Craig, C. L., Coddington, J. A. and Elgar, M. A. (2000). The functional significance of silk decorations of orb-web spiders: a critical review of the empirical evidence. *Biol. Rev.* **75**, 649-669.

ImageJ (2006). Online manual for the WCIF-ImageJ collection. http://www.uhnresearch.ca/facilities/wcif/imagej/.

Israelachvili, J. N. (1992). *Intermolecular and Surface Forces*. Santa Barbara: Academic Press.

Opell, B. D. (1994a). The ability of spider cribellar prey capture thread to hold insects with different surface features. *Funct. Ecol.* **8**, 145-150.

Opell, B. D. (1994b). Factors governing the stickiness of cribellar prey capture threads in the spider family Uloboridae. *J. Morphol.* **221**, 111-119.

Opell, B. D. (1994c). Increased stickiness of prey capture threads accompanying web reduction in the spider family Uloboridae. *Funct. Ecol.* **8**, 85-90.

Opell, B. D. (1997). The material cost and stickiness of capture threads and the evolution of orb-weaving spiders. *Biol. J. Linn. Soc. Lond.* **62**, 443-458.

Opell, B. D. (1998). Economics of spider orb-webs: the benefits of producing adhesive capture thread and of recycling silk. *Funct. Ecol.* **12**, 613-624.

Opell, B. D. (1999a). Changes in spinning anatomy and thread stickiness associated with the origin of orb-weaving spiders. *Biol. J. Linn. Soc. Lond.* **68**, 593-612.

Opell, B. D. (1999b). Redesigning spider webs: stickiness, capture area and the evolution of modern orb-webs. *Evol. Ecol. Res.* **1**, 503-516.

Opell, B. D. (2002). Estimating the stickiness of individual adhesive capture threads in spider orb-webs. *J. Arachnol.* **30**, 494-502.

Opell, B. D. and Hendricks, M. L. (2007). Adhesive recruitment by the viscous capture threads of araneoid orb-weaving spiders. *J. Exp. Biol.* **210**, 553-560.

Opell, B. D., Bond, J. E. and Warner, D. A. (2006). The effects of capture spiral composition and orb-web orientation on prey interception. *Zoology* **109**, 339-345.

Peters, H. M. (1984). The spinning apparatus of Uloboridae in relation to the structure and construction of capture threads (Arachnida, Araneida). *Zoomorphology* **104**, 96-104.

Peters, H. M. (1986). Fine structure and function of capture threads. In *Ecophysiology of Spiders* (ed. W. Nentwig), pp. 187-202. New York: Springer-Verlag.

Peters, H. M. (1995). Ultrastructure of orb spiders' gluey capture threads. *Naturwissenschaften* **82**, 380-382.

Reichert, S. E. and Cady, A. B. (1983). Patterns of resource use and tests for competitive release in a spider community. *Ecology* **64**, 899-913.

Tillinghast, E. K., Townley, M. A., Wight, T. N., Uhlenbruck, G. and Janssen, E. (1993). The adhesive glycoprotein of the orb-web of *Argiope aurantia* (Araneae, Araneidae). *Mater. Res. Soc. Symp. Proc.* **292**, 9-23.

Townley, M. A., Bernstein, D. T., Gallanger, K. S. and Tillinghast, E. K. (1991). Comparative study of orb-web hydroscopicity and adhesive spiral composition in three areneid spiders. *J. Exp. Zool.* **259**, 154-165.

Vollrath, F. and Tillinghast, E. K. (1991). Glycoprotein glue beneath a spider web's aqueous coat. *Naturwissenschaften* **78**, 557-559.

Vollrath, F., Fairbrother, W. J., Williams, R. J. P., Tillinghast, E. K., Bernstein, D. T., Gallagher, K. S. and Townley, M. A. (1990). Compounds in the droplets of the orb spider's viscid spiral. *Nature* **345**, 526-528.

Wise, D. H. (1993). *Spiders in Ecological Webs.* New York: Cambridge University Press.

Wise, D. H. and Barata, J. L. (1983). Prey of two syntopic spiders with different web structures. *J. Arachnol.* **11**, 271-281.

Zschokke, S. (2002). Ultraviolet reflectance of spiders and their webs. *J. Arachnol.* **30**, 246-254.